

## Graphical Abstract

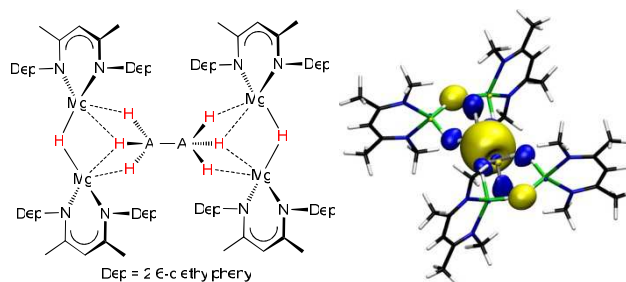
### Synthesis, Characterisation and Computational Analysis of the Dialanate Dianion,

### $[\text{H}_3\text{Al}-\text{AlH}_3]^{2-}$ : A Valence Isoelectronic Analogue of Ethane

Simon J. Bonyhady, Nicole Holzmann, Gernot Frenking,\* Andreas Stasch\* and Cameron

Jones\*

**HAlAl certified.** The first example of a binary, low oxidation state aluminium hydride species that is stable at ambient temperature, is reported (see picture). Computational studies reveal the stability of the aluminium(II) hydride dianion to be derived from its complexation with two bulky dimagnesium hydride cations.



**Keywords:** dialanate, metal-metal bonding, hydride, magnesium(I), DFT calculations.

Correspondence:

Prof. Cameron Jones

School of Chemistry

PO Box 23

Monash University

VIC, 3800

Australia

---

**Synthesis, Characterisation and Computational Analysis of the Dialanate Dianion,**

**$[\text{H}_3\text{Al}-\text{AlH}_3]^{2-}$ : A Valence Isoelectronic Analogue of Ethane**

**Simon J. Bonyhady,<sup>a</sup> Nicole Holzmann,<sup>b</sup> Gernot Frenking,<sup>\*,b</sup> Andreas Stasch<sup>\*,a</sup> and Cameron Jones<sup>\*,a</sup>**

[\*] Dr. S. J. Bonyhady, Dr. A. Stasch, Prof. C. Jones

School of Chemistry, PO Box 23

Monash University

VIC, 3800 (Australia)

E-mail: cameron.jones@monash.edu

Homepage: <http://www.monash.edu/science/research-groups/chemistry/jonesgroup>

Dr. N. Holzmann, Prof. G. Frenking

Fachbereich Chemie, Philipps-Universität Marburg

35032, Marburg (Germany)

E-mail: frenking@chemie.uni-marburg.de

Dr. A. Stasch

Current address: EaStCHEM School of Chemistry

University of St Andrews

North Haugh, KY16 9ST, St Andrews (UK)

E-mail: as411@st-andrews.ac.uk

E-mail: cameron.jones@monash.edu (CJ); as411@st-andrews.ac.uk (AS); frenking@chemie.uni-marburg.de (GF)

---

**Abstract:** The first example of a binary, low oxidation state aluminium hydride species that is stable at ambient temperature, *viz.* the dianion in  $[\{({}^{\text{Dep}}\text{Nacnac})\text{Mg}\}_2(\mu\text{-H})_2][\text{H}_3\text{Al-AlH}_3]$  ( ${}^{\text{Dep}}\text{Nacnac} = [(\text{DepNCMe})_2\text{CH}]^-$ , Dep = 2,6-diethylphenyl), has been prepared *via* a magnesium(I) reduction of the alanate complex,  $({}^{\text{Dep}}\text{Nacnac})\text{Mg}(\mu\text{-H})_3\text{AlH}(\text{NEt}_3)$ . An X-ray crystallographic analysis has shown the compound to be a contact ion complex, which computational studies have revealed to be the source of the stability of the aluminium(II) dianion.

---

The study of boron hydrides is of undoubted importance to inorganic chemistry, and numerous neutral and anionic examples of such compounds are now known, many of which exhibit one or more boron-boron bonds.<sup>[1]</sup> In contrast, the chemistry of binary aluminium hydrides is poorly developed, with the only isolated contributions to this compound class possessing aluminium centres in the +3 oxidation state, e.g. polymeric alane (AlH<sub>3</sub>)<sub>∞</sub> and the alanate anion [AlH<sub>4</sub>]<sup>-</sup>.<sup>[2]</sup> With that said, a number of other transiently stable alanes, exhibiting various aluminium oxidation states, have been studied in cryogenic matrices and the gas phase. These include AlH, AlH<sub>3</sub>, H<sub>2</sub>Al(μ-H)<sub>2</sub>AlH<sub>2</sub>, H<sub>2</sub>AlAlH<sub>2</sub> and the tetrahedral cluster Al<sub>4</sub>H<sub>6</sub>.<sup>[3]</sup> Given the intense current interest in utilising aluminium hydrides in hydrogen storage materials,<sup>[4]</sup> it would be of significant benefit to extend the ranks of these compounds to examples that are both stable under ambient conditions, and that incorporate low oxidation state aluminium centres.

Several years ago we demonstrated that low oxidation state aluminium hydride complexes could be readily accessed *via* reduction of aluminium(III) hydrides with β-diketiminato coordinated magnesium(I) dimers that were developed in our group. In one such reaction, treatment of an N-heterocyclic carbene (NHC) adduct of AlH<sub>3</sub> with {(<sup>Mes</sup>Nacnac)Mg-}<sub>2</sub> (<sup>Mes</sup>Nacnac = [(MesNCMe)<sub>2</sub>CH]<sup>-</sup>, Mes = mesityl) led to the thermally robust aluminium(II) hydride complex, **1** (Figure 1), which can be considered as an NHC adduct of the transient parent dialane(4), Al<sub>2</sub>H<sub>4</sub>.<sup>[5]</sup> It seemed to us that related magnesium(I) reductions of aluminium hydrides could lead to an expansion of the library of known low oxidation state alanes or alanates. One target we were particularly interested in was the dialanate, [H<sub>3</sub>Al–AlH<sub>3</sub>]<sup>2-</sup>, as (i) transition metal coordinated boron analogues of this dianion have been known for some time,<sup>[6]</sup> (ii) it is a valence isoelectronic analogue of ethane, and (iii) because a recent computational study has suggested the dialanate may be an experimentally isolable entity.<sup>[7]</sup> Here, we report on the synthesis of the dianion as a thermally stable contact ion complex with two dimagnesium hydride cations.

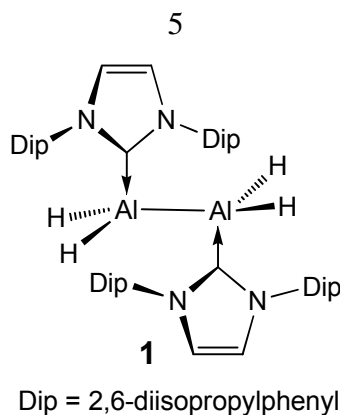
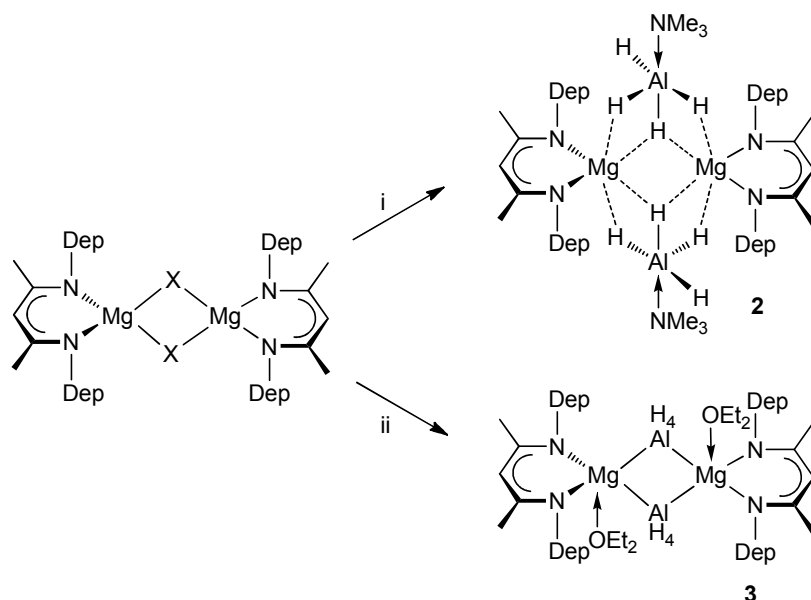


**Figure 1.** An N-heterocyclic carbene complex of  $\text{Al}_2\text{H}_4$ .

The magnesium(I) reduction of compounds incorporating the alanate anion,  $[\text{AlH}_4]^-$ , seemed to be a logical route to compounds containing the target dialanate dianion, based on the successful preparation of **1**. However, in order to stabilise the dialanate from undergoing disproportionation processes, it was believed a relatively large, Lewis acidic cation, that could form a contact ion complex with the dianion, would be required. To this end, the  $\beta$ -diketiminato magnesium alanate precursor complexes, **2** and **3**, were prepared *via* two routes (Scheme 1). In the first instance, treatment of the magnesium hydride complex,  $\{(\text{Dep}^{\text{Nacnac}})\text{Mg}(\mu\text{-H})\}_2$  ( $\text{Dep}^{\text{Nacnac}} = [(\text{DepNcMe})_2\text{CH}]^-$ , Dep = 2,6-diethylphenyl)<sup>[8]</sup> with  $\text{AlH}_3(\text{NMe}_3)$  afforded the trimethylamine coordinated alanate complex, **2**, in essentially quantitative yield. In contrast, the magnesium etherate complex, **3**, was formed in low-moderate yield *via* a salt elimination reaction between  $\{(\text{Dep}^{\text{Nacnac}})\text{Mg}(\mu\text{-Cl})\}_2$  (see SI for crystallographic details) and  $\text{Na}[\text{AlH}_4]$  in diethyl ether. It is noteworthy that attempts to cleanly remove the ether of coordination from **3** by gently heating the compound in the solid state under vacuum, then recrystallising the remaining solid from benzene, were largely unsuccessful. With that said, on one occasion several crystals of  $\{(\text{Dep}^{\text{Nacnac}})\text{Mg}(\mu\text{-AlH}_4)\}_2$  were obtained (see SI for crystallographic details), though in insufficient yield to explore the reduction of the compound, or obtain spectroscopic data for it.



**Scheme 1.** Preparation of compounds **2** and **3**; i) X = H, AlH<sub>3</sub>(NMe<sub>3</sub>); ii) X = Cl, Na[AlH<sub>4</sub>], OEt<sub>2</sub>, NaCl.

Both compounds **2** and **3** are thermally stable in the solid state. Their <sup>1</sup>H and <sup>13</sup>C{<sup>1</sup>H} NMR spectra suggest more symmetrical time averaged structures in solution than they possess in the solid state (see below). It is likely that this results from rapid breaking and reforming of Mg-H-Al bridges on the NMR timescale, though this could not be examined by variable temperature NMR studies due to the low solubility of the complexes in non-coordinating solvents at reduced temperatures. Broad hydride resonances were recorded for the compounds (**2** δ 3.14 ppm; **3** δ 2.75 ppm) from their <sup>1</sup>H NMR spectra (*cf.* δ 3.09 ppm for the alanate anion of [{MeN(C<sub>2</sub>H<sub>4</sub>NMe<sub>2</sub>)<sub>2</sub>AlH<sub>2</sub>][AlH<sub>4</sub>]<sup>[9]</sup>), while a very broad signal was observed in the <sup>27</sup>Al NMR spectrum of **3** only (C<sub>6</sub>D<sub>6</sub> solution: δ 108 ppm; *cf.* δ 110 ppm for Mg(AlH<sub>4</sub>)<sub>2</sub>(THF)<sub>4</sub><sup>[10]</sup>). The solid state IR spectra of the compounds display broad, strong bands (**2** ν 1834 cm<sup>-1</sup>; **3** ν 1841 cm<sup>-1</sup>; *cf.* ν 1863 cm<sup>-1</sup> for {Cp<sub>2</sub>Y(μ-H)<sub>2</sub>AlH<sub>2</sub>(NEt<sub>3</sub>)<sub>2</sub><sup>[11]</sup>) which were assigned to terminal Al-H stretching modes, while it is likely the Al-H-Mg stretching modes are masked by ligand absorptions.

An X-ray crystallographic analysis of **2** was carried out, and the molecular structure of the compound is depicted in Figure 2. Due to the poor quality of the diffraction data for **3**, its structure is not included here, but preliminary refinements clearly showed that it is a dimer in the solid state,

with  $\text{AlH}_4$  units bridging  $(^{\text{Dep}}\text{Nacnac})\text{Mg}$  fragments. This likely occurs through Al-H-Mg linkages, though the nature of this bridging is not well-defined due to the poor quality of the structure. The location of the hydride ligands of **2** from difference maps, revealed a similar situation for that compound, in that two  $[\text{AlH}_4(\text{NMe}_3)]$  moieties bridge magnesium centres through three Al-H-Mg linkages, leaving one terminal Al-H bond. This is a similar situation to that in the related yttrium compound,  $\{\text{Cp}_2\text{Y}(\mu\text{-H})_2\text{AlH}_2(\text{THF})\}_2$ <sup>[11]</sup>, and results in the Al centres having distorted trigonal bipyramidal geometries with three hydrides in equatorial positions, and hydride/ $\text{NMe}_3$  ligands axial. The three Al- $\text{H}_{\text{eq}}$  distances are in the normal range for such interactions,<sup>[12]</sup> though the terminal Al-H separation is, not surprisingly, shortest. Interestingly, the Al- $\text{H}_{\text{ax}}$  distance is markedly larger (by  $> 0.3 \text{ \AA}$ ) than for the other bonds, probably because the axial hydrides also bridge both Lewis acidic Mg centres (mean Mg- $\text{H}_{\text{ax}}$  distance:  $2.005 \text{ \AA}$ ; cf.  $1.965 \text{ \AA}$  mean in  $\{(^{\text{Dep}}\text{Nacnac})\text{Mg}(\mu\text{-H})\}_2$ <sup>[8]</sup>).

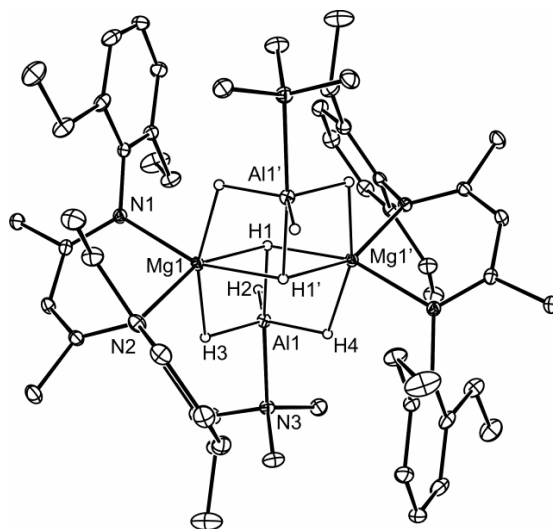
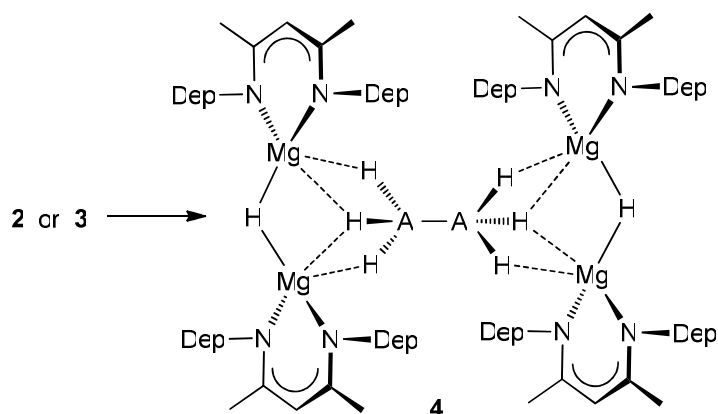


**Figure 2.** Molecular structure of **2** (25% thermal ellipsoids; hydrogen atoms, except hydrides, omitted). Selected bond lengths ( $\text{\AA}$ ) and angles ( $^\circ$ ): Al(1)-N(3) 2.1216(14), Al(1)-H(1) 1.89(2), Al(1)-H(3) 1.56(2), Al(1)-H(4) 1.557(19), Al(1)-H(2) 1.500(19), Mg(1)-H(1) 2.02(2), Mg(1)-H(3) 2.14(2), N(1)-Mg(1)-N(2) 92.52(5), H(1)-Mg(1)-H(1)' 73.2(9), N(3)-Al(1)-H(1) 171.4(6), H(3)-Al(1)-H(4) 112.9(10), H(3)-Al(1)-H(2) 122.4(10), H(4)-Al(1)-H(2) 124.4(10),

With compound **2** in hand, its reduction with a slight excess of the magnesium(I) reducing agent,  $\{(^{\text{Dep}}\text{Nacnac})\text{Mg}\}_2$ <sup>[8]</sup> in a toluene solution was examined (Scheme 2). This led to a low

isolated yield (24%) of the dialanate complex, **4**, as a colourless crystalline solid. Following the reaction by  $^1\text{H}$  NMR spectroscopy showed that the compound is generated in higher yields (*ca.* 70%) in solution, prior to isolation. In contrast, related reductions of **3** with  $\{({}^{\text{Dep}}\text{Nacnac})\text{Mg}\}_2$  were not as clean, though small amounts of **4** (*ca.* 10% yield) were observed in  $^1\text{H}$  NMR spectra of reaction mixtures. As a result, this route to **4** was not pursued further.



**Scheme 2.** Preparation of dialanate complex **4**; i)  $\{({}^{\text{Dep}}\text{Nacnac})\text{Mg}\}_2$ , -  $\text{OEt}_2$  or -  $\text{NMe}_3$ .

Compound **4** is remarkably stable in the solid state (decomp. 234-236 °C), and does not show any evidence of decomposition in benzene solutions at ambient temperature over several days. The  $^1\text{H}$  and  $^{13}\text{C}\{^1\text{H}\}$  NMR spectra of **4** are simpler than would be expected if the molecule retains its solid state structure in solution. For example, only one set of ethyl resonances are seen in both spectra, implying a fluxional process is in operation. This likely involves breaking and reforming of the  $\text{Mg}\cdots(\mu\text{-H})\text{Al}$  interactions, which is rapid on the NMR timescale. Such a process could also provide an explanation as to why no aluminium or magnesium hydride resonances were seen in the  $^1\text{H}$  NMR spectrum of **4**. These resonances are typically broad, and could be broadened further due to the fluxionality of **4** in solution. Similarly no resonance was observed in the  $^{27}\text{Al}\{^1\text{H}\}$  NMR spectrum of the compound. Furthermore, no Al-H or Mg-H stretching bands could be assigned in the solid state IR spectrum of **4**, which is not surprising, as these would be expected in the fingerprint region, and thus hard to distinguish from ligand stretching bands. Due to synthetic limitations, the synthesis of the octa-deuteride analogue of **4** was not attempted.



So as to confirm the formulation of **4** in the solid state, the X-ray crystal structure of the compound was determined (Figure 3). The location of all hydride ligands from difference maps, and the free refinement of their positional parameters, allows a discussion of the geometry of the compound. It is a dimer with an unsupported Al-Al bond, the length of which (2.548(1) Å) is at the lower end of the known range for such interactions.<sup>[12]</sup> It is also considerably shorter than in the neutral dialane(4) complex, **1** (2.635(8) Å),<sup>[5]</sup> and Uhl's alkyl/hydrido substituted aluminium(II) anion,  $[\text{R}_2(\text{H})\text{Al}-\text{AlR}_2]^-$  (2.667(3) Å, R = C(H)(SiMe<sub>3</sub>)<sub>2</sub>).<sup>[13]</sup> Moreover, it is shorter than calculated for the contact ion complex,  $\text{Li}_2[\text{H}_3\text{Al}-\text{AlH}_3]$  (2.69 Å),<sup>[7]</sup> in which the lithium ions each bridge hydrides bound to adjacent aluminium centres. In contrast, in **4**, both Mg centres of each  $[\{(\text{DepNacnac})\text{Mg}\}_2(\mu\text{-H})]^+$  cation are ligated by hydrides that are attached to a single aluminium centre. This situation undoubtedly helps to stabilise the  $[\text{H}_3\text{Al}-\text{AlH}_3]^{2-}$  dianion, the metal centres of which have distorted tetrahedral geometries. Although the positions of the hydride centres were not located with a high degree of accuracy, it is clear that all the Al-H and Mg-H distances lie in the normal ranges (*cf.* **2** and  $\{(\text{DepNacnac})\text{Mg}(\mu\text{-H})\}_2$ <sup>[8]</sup>). It is noteworthy that a variety of complexes related to **4**, but containing  $[\text{H}_3\text{B}-\text{BH}_3]^{2-}$  dianions, have been crystallographically characterised, but the B-B bonds of these are invariably supported through hydride bridges to transition metal centres.<sup>[4]</sup> Furthermore, as  $[\text{H}_3\text{Al}-\text{AlH}_3]^{2-}$  is valence isoelectronic to ethane, the lowest energy conformation of which is staggered, it is germane that the dianion also adopts a staggered conformation (*cf.* eclipsed  $\text{Li}_2[\text{H}_3\text{Al}-\text{AlH}_3]$ <sup>[7]</sup>). However, steric interactions between the two  $[\{(\text{DepNacnac})\text{Mg}\}_2(\mu\text{-H})]^+$  cations must contribute significantly to this situation.

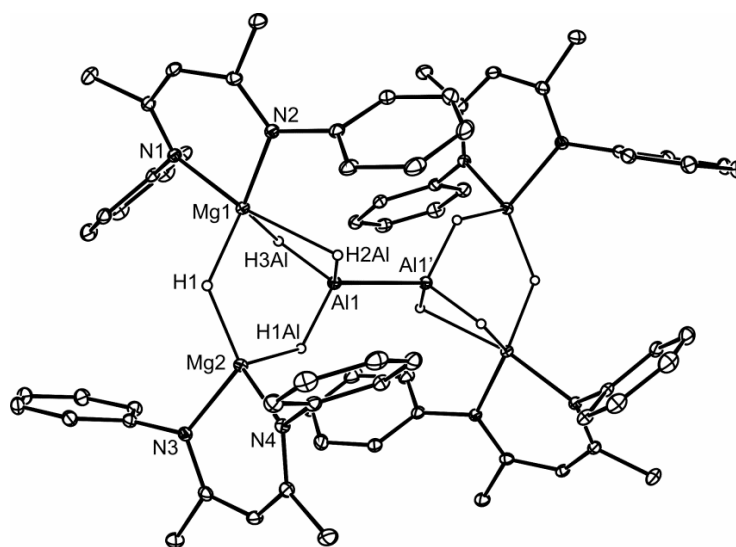


**Figure 3.** Molecular structure of **4** (25% thermal ellipsoids; hydrogen atoms, except hydrides, omitted). Selected bond lengths (Å) and angles (°) with calculated numbers at RI-BP86/def2-TZVPP in brackets: Al(1)-Al(1') 2.5479(9) [2.605], Al(1)-H(3Al) 1.563(18) [1.700], Al(1)-H(2Al) 1.537(19) [1.652], Al(1)-H(1Al) 1.606(19) [1.700], Mg(1)-H(1) 1.91(2) [1.837], Mg(1)-H(3Al) 1.988(18) [2.058], Mg(1)-H(2Al) 2.220(19) [2.217], Mg(2)-H(1) 1.82(2) [1.907], Mg(2)-H(1Al) 1.926(19) [1.943], Al(1')-Al(1)-H(3Al) 118.0(7) [120.2], Al(1')-Al(1)-H(2Al) 121.7(7) [121.9], Al(1')-Al(1)-H(1Al) 117.4(7) [115.3], H(3Al)-Mg(1)-H(2Al) 64.0(7) [68.7], H(3Al)-Mg(1)-H(1) 99.7(8) [97.1], H(2Al)-Mg(1)-H(1) 86.5(8) [97.1], H(1Al)-Mg(2)-H(1) 103.0(8) [100.0], Mg(1)-H(1)-Mg(2) 125(1) [130.6].

We carried out quantum chemical calculations using density functional theory (DFT) at the RI-BP86/def2-TZVPP level in order to elucidate the bonding situation of the dialanate complex **4**. Details of the method are provided in Supporting Information. Figure 3 shows that the calculated bond lengths and angles are in reasonable agreement with experiment. There are some larger deviations for the metal-hydrogen bonds, which is at least partly due to the low accuracy of the hydride ligand positions determined by X-ray crystallography (see SI for full details).

The analysis of the electronic structure indicates that **4** may rightfully be considered as a complex where a  $\text{Al}_2\text{H}_6^{2-}$  moiety is stabilized by two cations  $[\{(\text{DepNacnac})\text{Mg}\}_2(\mu\text{-H})]^+$ . NBO calculations of the atomic partial charges suggest that the  $\text{Al}_2\text{H}_6$  fragment carries a negative charge

of -1.24 e. The electronic charge is located at the hydrogen atoms while the aluminium atoms are positively charged (See Table S3 in SI). This means that there is a formal charge transfer of 0.76 e from  $\text{Al}_2\text{H}_6^{2-}$  to two cations,  $[\{(\text{DepNacnac})\text{Mg}\}_2(\mu\text{-H})]^+$ . Calculation of free  $\text{Al}_2\text{H}_6^{2-}$  at RI-BP86/def2-TZVPP gives a structure with an Al-Al distance of 2.723 Å, somewhat longer than in **4** (2.605 Å). However, free  $\text{Al}_2\text{H}_6^{2-}$  is only metastable while **4** is calculated to be thermodynamically stable with regard to breaking the Al-Al bond. Fission of the Al-Al bond in  $\text{Al}_2\text{H}_6^{2-}$ , giving two  $\text{AlH}_3^-$  anions, is exothermic with  $D_e = -29.1$  kcal/mol. In contrast, the dissociation of **4** leading to two radicals  $\cdot\text{AlH}_3[\{(\text{DepNacnac})\text{Mg}\}_2(\mu\text{-H})]$  is endothermic with  $D_e = 52.4$  kcal/mol. The latter value increases strongly when dispersion forces are considered. Calculations of the bond dissociation energy (BDE) of **4** using Grimme's D3 term for dispersion forces at RI-BP86-D3(BJ)/def2-TZVPP using the RI-BP86/def2-TZVPP optimized geometries gives  $D_e = 115.2$  kcal/mol. Thus, compound **4** is stabilized by the direct interactions between the  $\text{Al}_2\text{H}_6^{2-}$  moiety and the cations,  $[\{(\text{DepNacnac})\text{Mg}\}_2(\mu\text{-H})]^+$ . The stabilization is further enhanced by dispersion forces.

For the bonding analysis in **4** we used a model compound **4M** where the bulky Dep groups on the  $\text{DepNacnac}$  ligands are replaced by methyl groups, to give the smaller  $\beta$ -diketimate,  $\text{MeNacnac}$ . The optimized geometry of **4M** is very similar to that of **4** (see SI). The calculated bond order for the Al-Al bond in **4M** is  $P(\text{Al-Al}) = 0.96$ , which indicates a single bond. Figure 4a shows the HOMO-4 of **4M**, which is easily identified as a Al-Al bonding orbital. The higher-lying four MOs, which are energetically nearly degenerate, are delocalized over the four Nacnac rings, respectively (Fig. S3 in SI). We studied the interactions between the  $\text{Al}_2\text{H}_6^{2-}$  moiety and the  $[\{(\text{MeNacnac})\text{Mg}\}_2(\mu\text{-H})]^+$  units with an energy decomposition analysis (EDA-NOCV),<sup>[14]</sup> which allows the decomposition of the orbital interactions into pairwise contributions. The total orbital interactions of  $\Delta E_{\text{orb}} = -115.8$  kcal/mol are composed of several pairwise components. Figures 4b – 4d show the strongest orbital interaction of  $\Delta E_1 = -21.4$  kcal/mol which takes place between the HOMO of  $\text{Al}_2\text{H}_6^{2-}$  and the LUMO of the  $[\{(\text{MeNacnac})\text{Mg}\}_2(\mu\text{-H})]^+$  units. The associated charge flow is displayed in Fig. 4d. The colour coding red  $\rightarrow$  blue illustrates that electronic charge is

donated from the  $\text{Al}_2\text{H}_6^{2-}$  fragment to the Nacnac ligands of **4M**. Further orbital contributions come from lower-lying MOs of  $\text{Al}_2\text{H}_6^{2-}$  to the magnesium cation scaffold.

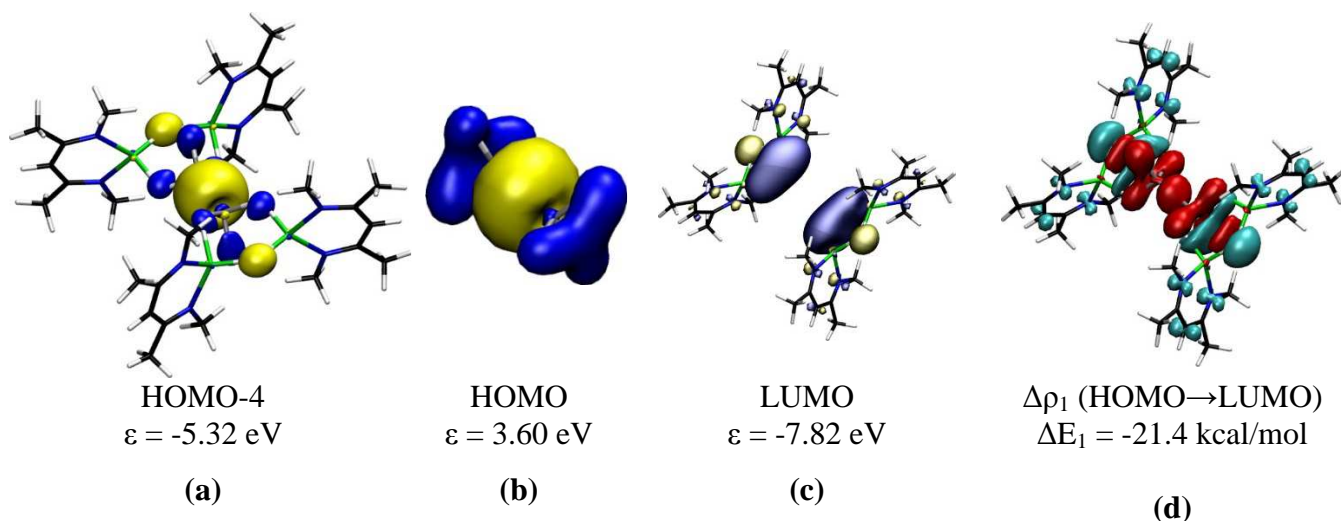


**Figure 4.** (a) HOMO-4 of compound **4M**. (b) HOMO of  $\text{Al}_2\text{H}_6^{2-}$ . (c) LUMO of the two  $[\{(\text{Me})\text{Nacnac}\}\text{Mg}\}_2(\mu\text{-H})^+$  cations. (d) Deformation density  $\Delta\rho_1$  showing the associated charge flow HOMO  $\rightarrow$  LUMO (red  $\rightarrow$  blue) which lowers the energy by  $\Delta E_1 = -21.4$  kcal/mol.

In summary, the first example of a binary, low oxidation state aluminium hydride species that is stable at ambient temperature, *viz.*  $[\text{H}_3\text{Al}-\text{AlH}_3]^{2-}$ , has been prepared *via* magnesium(I) reduction of an alanate,  $[\text{AlH}_4]^-$ , complex. Computational studies revealed that the stability of the dianion, a valence isoelectronic analogue of ethane, is derived from its coordination to two bulky cations,  $[\{(\text{Dep})\text{Nacnac}\}\text{Mg}\}_2(\mu\text{-H})^+$ . We continue to explore the chemistry of low oxidation state aluminium hydride compounds, which hold potential as models for the study of aluminium based hydrogen storage materials.

### Acknowledgement

CJ and AS gratefully acknowledge financial support from the Australian Research Council, while CJ thanks the U.S. Air Force Asian Office of Aerospace Research and Development (FA2386-14-1-4043) for funding. GF acknowledges financial support from the Deutsche Forschungsgemeinschaft.

Part of this research was undertaken on the MX1 beamline at the Australian Synchrotron, Victoria, Australia.

## Experimental Section

Full synthetic, spectroscopic and crystallographic details for new compounds; and full details and references for the DFT calculations can be found in the Supporting Information.

## Notes and References

- [1] See for example: (a) R. B. King, *Chem. Rev.* **2001**, *101*, 1119-1152; (b) F. A. Cotton, G. Wilkinson, C. A. Murillo, M. Bochmann, *Advanced Inorganic Chemistry*, Wiley, Chichester, United Kingdom, 6th ed., **1999**.
- [2] S. Aldridge, A. J. Downs, *Chem. Rev.* **2001**, *101*, 3305-3366.
- [3] See for example: (a) X. Li, A. Grubisic, S. T. Stokes, J. Cordes, G. F. Ganteför, K. H. Bowen, *Science* **2006**, *315*, 356-358; (a) A. Grubisic, X. Li, S. T. Stokes, J. Cordes, G. F. Ganteför, K. H. Bowen, B. Kiran, P. Jena, R. Burgert, H. Schnöckel, *J. Am. Chem. Soc.* **2007**, *129*, 5969-5975; (c) X. Weng, L. Andrews, S. Tam, M. E. DeRose, M. E. Fajardo, M. E., *J. Am. Chem. Soc.* **2003**, *125*, 9218-9228.
- [4] See for example: (a) J. Graetz, J. J. Reilly, V. A. Yartys, J. P. Maehlen, B. M. Bulychev, V. E. Antonov, B. P. Tarasov, I. E. Gabis, *J. Alloys Compd.* **2011**, *509*, S517-S528; (b) R. Zidan, B. L. Garcia-Diaz, C. S. Fewox, A. C. Stowe, J. R. Gray, A. G. Harter, *Chem. Commun.* **2009**, 3717-3719; A. Andreason, *Int. J. Hydrogen Energy* **2008**, *33*, 7489-7497.
- [5] S. J. Bonyhady, D. Collis, G. Frenking, N. Holzmann, C. Jones, A. Stasch, *Nature Chem.* **2010**, *2*, 865-869.
- [6] See for example: (a) D. Sharmila, B. Mondal, R. Ramalakshmi, S. Kundu, B. Varghese, S. Ghosh, *Chem. Eur. J.*, 2015, **21**, 5074-5083; (b) S. K. Bose, K. Geetharani, V. Ramkumar, S. M. Mobin, S. Ghosh, *Chem. Eur. J.* **2009**, *15*, 13483-13490.
- [7] J. T. Gish, I. A. Popov, A. I. Boldyrev, *Chem. Eur. J.* **2015**, *21*, 5307-5310.

- [8] R. Lalrempuia, C. E. Kefalidis, S. J. Bonyhady, B. Schwarze, L. Maron, A. Stasch, C. Jones, *J. Am. Chem. Soc.* **2015**, *137*, 8944-8947.
- [9] J. L. Atwood, K. D. Robinson, C. Jones, C. L. Raston, *J. Chem. Soc., Chem. Commun.* **1991**, 1697-1699.
- [10] H. Noth, M. Schmidt, A. Treitl, *Chem. Ber.* **1995**, *128*, 999-1006.
- [11] V. K. Belsky, A. B. Erofeev, B. M. Bulychev, G. L. Soloveichik, *J. Organomet. Chem.* **1984**, *265*, 123-133.
- [12] As determined from a survey of the Cambridge Crystallographic Database, September, 2016.
- [13] W. Uhl, A. Vester, *Chem. Ber.* **1993**, *126*, 941-945.
- [14] A. Michalak, M. Mitoraj, T. J. Ziegler, *Phys. Chem. A.* **2008**, *112*, 1933-1939.